MERCURIC IODIDE CRYSTAL GROWTH AND FRISCH COLLAR DETECTOR FABRICATION

MATERIALS FOR NUCLEAR SYSTEMS

KEYWORDS: *HgI_2, Faile method, Frisch collar devices*

E. ARIESANTI,[a]* A. KARGAR,[b] and D. S. McGREGOR[a]

[a]*Kansas State University, S.M.A.R.T. Laboratory, Manhattan, Kansas 66506*
[b]*Radiation Monitoring Devices, Inc., 44 Hunt Street, Watertown, Massachusetts 02172*

Received April 19, 2010
Accepted for Publication October 18, 2010

Being a high-Z material, mercuric iodide (HgI_2) has a relatively high gamma-ray absorption coefficient. Its low charge carrier mobilities, however, have somewhat hampered the interest in using this material as a room-temperature gamma-ray spectrometer. By using the Frisch collar technology, the influence of the low charge carrier can be significantly reduced. The growth of HgI_2 by the Faile method in a horizontal furnace fortuitously produces tetragonal prismatic crystals. These crystals with appropriate dimensions can be fabricated into Frisch collar spectrometers. With the Frisch collar technology, 1.8% energy resolution for 662-keV gamma rays has been achieved.

I. INTRODUCTION

Mercuric iodide (HgI_2) is considered as a candidate material for room-temperature gamma-ray detectors because of its high-Z constituents and a band gap that is relatively wide (~2.13 eV). Despite these favorable properties, HgI_2 suffers from several detrimental attributes, such as low charge carrier mobilities ($\mu_e \sim 100$ cm·V^{-1}·s^{-1}, $\mu_h \sim 8$ cm·V^{-1}·s^{-1} for HgI_2 as compared to $\mu_e \sim 1000$ cm·V^{-1}·s^{-1}, $\mu_h \sim 150$ cm·V^{-1}·s^{-1} for CdZnTe) (Ref. 1) and low yield strength.[2] With low mobilities, charge carriers are prone to be captured in traps. Holes, which have a lower mobility than electrons do, are more easily trapped. Unfortunately, the influence of trapped charges is compromised, and their contribution to charge induction is diminished. Low yield strength due to the weak van der Waals bonds between iodine layers normal to the [001] axis leads to plastic deformation.[2] Hence, HgI_2 crystals must be handled and processed carefully. These drawbacks, unfortunately, have prevented a wider use of HgI_2 single crystals as room-temperature gamma-ray detectors.

Removal of the hole contribution from the charge induction process will improve energy resolution. One detector design that excludes much of the hole contribution is the Frisch collar detector design.[3–5] Recent results of cadmium zinc telluride (CdZnTe) detectors fabricated with the Frisch collar design have shown excellent energy resolution.[5–7] Sub-1% energy resolution is consistently achieved with CdZnTe Frisch collar detectors. A CdZnTe Frisch collar detector consists of a CdZnTe crystal cut and polished into a right square prism (i.e., a tetragonal prism). The crystal is then wrapped with a Teflon tape (a low dielectric material) and a copper shim (as the conductive collar). This Frisch collar detector is operated with the copper collar and cathode held at zero potential while the anode is at a positive potential.

While the Frisch collar detector design is ideal for HgI_2, the issue of carefully handling and processing of the crystal remains. The most widely used method for growing HgI_2 is vapor growth in a vertical furnace.[8] This method, also commonly known as the modified Scholz method,[9] was used to grow HgI_2 bulk single crystals weighing between 100 and 200 g within 1 to 2 months. Although much material is harvested at the end of the growth period, not all parts of the grown crystal are suitable for detector fabrication. Consequently, various fabrication processes must be used to cut and shape the crystal. With the use of many fabrication steps, however, the chances for crystal deformation and impurity

*E-mail: ancilla@ksu.edu

incorporation increase. Previous attempts in using a cut-and-shaped HgI_2 crystal to fabricate a Frisch collar detector demonstrated a spectrometer only with limited success.[10]

The vapor growth method introduced by Faile et al.[11] can produce crystals of the ideal size and shape for Frisch collar detectors. The Faile method utilizes polymer added in the growth ampoule and is performed in a horizontal furnace. The addition of polymer has been shown to affect the habit of the grown crystals. Without the addition of organics, the {h0l} faces appear along with the more prominent (001) and {110} faces. *With* the addition of organics, specifically low molecular weight polyethylene, the areas of {h0l} faces are severely reduced, giving the overall crystal shape of tetragonal prisms with the length parallel to the [001] axis. In the past, efforts to determine the causes for this habit modification focused on the effect of added polymer on mass transport, purification, and HgI_2 stoichiometry.[12–15] To date, however, none of these efforts have satisfactorily explained the effect of polymer addition in modifying the HgI_2 crystal habit.

The current objectives of the HgI_2 research in the Semiconductor Materials and Radiological Technologies (S.M.A.R.T.) Laboratory at Kansas State University are the following: (a) to determine the effects of polyethylene in HgI_2 crystal habit modification, (b) to fabricate HgI_2 Frisch collar detectors, and (c) to characterize the polarization behavior of the detectors. A review of HgI_2 growth and HgI_2 Frisch collar detector research at Kansas State University is presented in this study.

II. THEORY

II.A. α-HgI_2

Several crystal structures of HgI_2 have been observed,[16,17] with α-HgI_2 as the most stable structure at ambient temperatures.[18] The space group designation for α-HgI_2 is $P4_2/nmc$ (Ref. 19). It has a tetragonal crystal structure with crystal parameters $a = b = 4.316$ Å and $c = 12.450$ Å. The crystal structure is considered a layered structure, with the adjacent layers (stacked along the [001] axis) being held together by weak van der Waals bonds (Fig. 1). Because of the anisotropy in crystal parameters, the properties of α-HgI_2 are expected to be direction dependent. For example, $\mu_{e,h,[001]}$ are not necessarily the same as $\mu_{e,h,\perp[001]}$. To date, however, only $\mu_{e,h,[001]}$ have been measured, with $\mu_{h,[001]}$ about one order of magnitude smaller than $\mu_{e,[001]}$ (Ref. 1).

II.B. Shockley-Ramo Theorem

Suppose that a gamma ray undergoes a photoelectric absorption at position $\vec{r}$ and a number of electron-hole pairs (for a total of initial charge Q_o) are created. Because of the presence of the electric field, these charges move toward their respective electrodes. As these charges are moving, an induced current due to the motion of these charges can be monitored at a chosen conductor (in this case, at the anode). The induced current can be solved using the concept of the weighting potential, which is derived from first principles using Green's second identity (i.e., Green's theorem).[20] Integrating the induced current produces the induced charge measured from the radiation event. The weighting potential concept has been used by Shockley[21] and Ramo[22] to solve the induced current due to a moving charge in a vacuum tube. The concept has also been used to determine the induced charge in semiconductor detectors.[23–25]

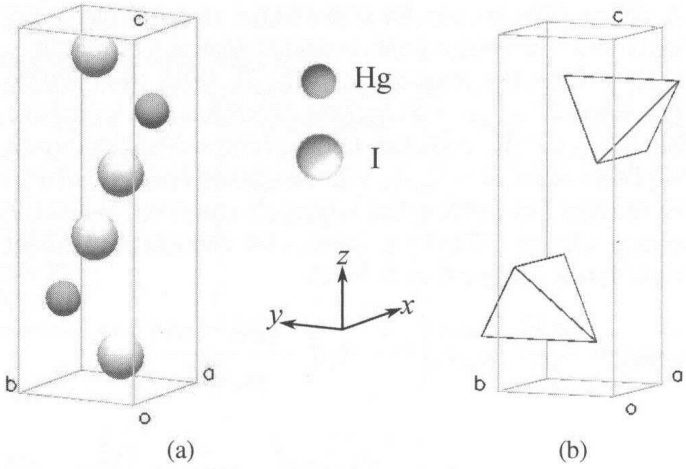

Fig. 1. (a) The α-HgI_2 unit cell consisting of two complete HgI_2 molecules. (b) The Hg and I ions form tetrahedral layers.

According to Ramo's theorem[22] the induced current due to a charge Q_o moving at velocity $\vec{v}(\vec{r})$ is

$$I(\vec{r}) = Q_o \vec{E}_w(\vec{r}) \cdot \vec{v}(\vec{r}) \ , \tag{1}$$

where $\vec{E}_w(\vec{r})$ is called the weighting field. The change in induced charge $dQ(\vec{r})$ with respect to time can be derived from Eq. (1) as

$$\frac{dQ(\vec{r})}{dt} = -Q_o \nabla V_w(\vec{r}) \cdot \frac{d\vec{r}}{dt} \ , \tag{2}$$

where $I(\vec{r}) \equiv dQ(\vec{r})/dt$ and $V_w(\vec{r})$ is the weighting potential. The weighting potential $V_w(\vec{r})$ can be defined simply as the actual potential at $\vec{r}$, $V(\vec{r})$, in a medium with no stationary charges or $\rho = 0$, normalized to the potential at the collecting or monitoring electrode.[26]

II.C. Planar Detector

Because of the tetragonal prismatic shape of the HgI_2 device, the physics of the HgI_2 planar device can be explained with Cartesian coordinates in one dimension.[7]

A planar detector can be represented as a parallel plate capacitor bounding a semiconductor material of length L, with a dielectric constant κ (Fig. 2). With the cathode grounded ($V_{cathode} = 0$) and the anode held at a positive bias ($V_{anode} = V_a > 0$), the electric field within the device is $|\vec{E}(\vec{x})| = E(x) = V_a/L$. The weighting field $\vec{E}_w(\vec{x})$ can be obtained by solving the Laplace's equation. When the charge carrier trapping is taken into account, the Hecht equation is obtained as follows:

$$Q(x) = \frac{Q_o V_a}{L^2}\left[\mu_e\tau_e\left(1 - \exp\left(-\frac{L(L-x)}{\mu_e\tau_e V_a}\right)\right) + \mu_h\tau_h\left(1 - \exp\left(-\frac{xL}{\mu_h\tau_h V_a}\right)\right)\right] . \quad (3)$$

The charge collection efficiency (CCE), $CCE(x)$, which is a measure of the uniformity of the detector response to gamma rays, can be obtained by taking the ratio of $Q(x)$ to Q_o.

II.D. Frisch Collar Detector

The physics and performance of the Frisch collar device have been thoroughly explained in the literature.[3,7] Figure 3 shows the cross section of a Frisch collar device. The Frisch collar is either grounded or biased at a potential between ground and the collecting electrode's bias. The Frisch collar of the device used in this study was coupled to the grounded cathode. Therefore, the analysis for the device reduces from a three-terminal device to a two-terminal device as in the planar device configuration. Furthermore, the device can be analyzed along its central line. Hence, the analysis is reduced to one-dimensional analysis, as in the planar device configuration. Ramo's theorem can again be used to solve the induced current in the Frisch collar device. A numerical analysis method, however, must be used to solve both the Laplace and the Poisson equations to obtain the weighting field $\vec{E}_w(\vec{x})$ and the actual electric field $\vec{E}(\vec{x})$, respectively.[7]

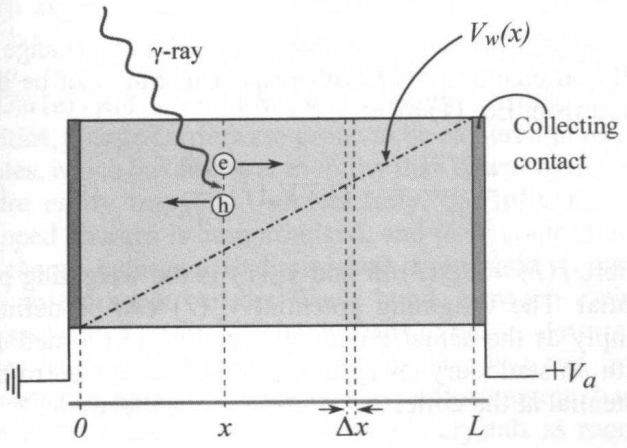

Fig. 2. Planar device configuration and the respective weighting potential $V_w(x)$. Since $dV_w(x)/dx$ is constant everywhere, for any incremental distance Δx, both electron and hole induce the same amount of change in induced charge.

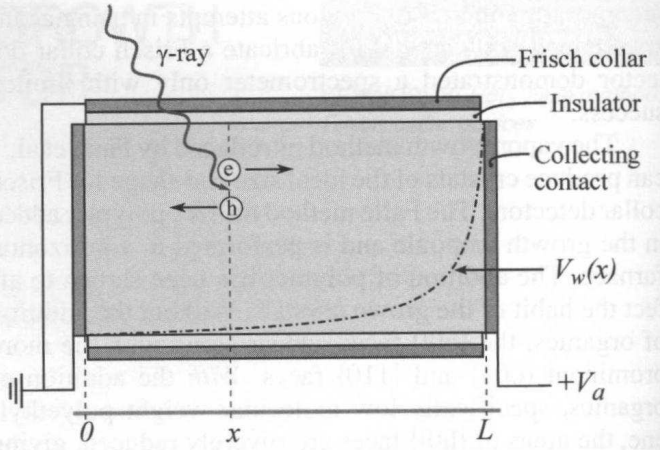

Fig. 3. Frisch collar device configuration and the respective weighting potential $V_w(x)$. Since $dV_w(x)/dx$ is larger toward the anode, the induced charge is attributed mostly to the motion of electrons as they travel toward the anode.

III. EXPERIMENTAL METHODS

III.A. Organics-Aided Growth of HgI_2

Purified HgI_2 was used as the starting material because the purity of the starting material has been shown to affect crystal morphology.[11,14] The starting HgI_2 (obtained from EG&G) was purified in a succession of purification stages as listed in Table I. These stages of purification were first implemented by EG&G to purify starting HgI_2 for growth in the vertical furnace.[27] In the S.M.A.R.T. Laboratory at Kansas State University the purification by sublimation in dynamic vacuum was completed in a one-zone furnace connected to a turbopump. The temperature utilized for the process was 140°C, and the process was repeated three times. The purified material was retrieved and placed in a double-chamber ampoule for melting at 350°C. The melting stage was followed by sublimation in static vacuum in the same ampoule at 140°C. The purified HgI_2 was retrieved by sublimation in dynamic vacuum.

Purified HgI_2 was placed in an ampoule and was mixed with a low $\overline{M}_w$ polyethylene. The ampoule was subsequently sealed under vacuum to $\sim 1 \times 10^{-4}$ Torr. The ampoule was then positioned in a two-zone horizontal furnace. The source was placed in the source zone (set at 230°C), and the deposition zone was set at 150°C. The

TABLE I

Purification Stages in Processing Starting HgI_2 Material

Purification Stage	Vacuum Level (Torr, Room Temperature)	Temperature (°C)	Iteration Number
Sublimation in dynamic vacuum	$\sim 5 \times 10^{-3}$	140	3
Melting	$\sim 1 \times 10^{-4}$	350	1
Sublimation in static vacuum	$\sim 1 \times 10^{-4}$	140	1
Sublimation in dynamic vacuum for retrieval	$\sim 5 \times 10^{-3}$	140	1

preceding step is called the source-processing step. Sublimated HgI_2 was condensed at the end of the deposition region in the ampoule and then subsequently retrieved for growth. Retrieved HgI_2 was placed in a clean ampoule and sealed under vacuum in the same manner previously mentioned. This growth ampoule was placed in a two-zone ampoule, with the source zone set at 100°C and the deposition zone at 80°C. The growth procedure lasted for 5 days, but not all of the source material was spent.

III.B. HgI_2 Frisch Collar Detector Fabrication and Spectroscopy

Harvested HgI_2 crystals were used as-is to fabricate the Frisch collar detectors. Neither extensive cutting nor polishing were required to shape or prepare the crystals. Cleaving the crystal with a razor blade parallel to the (001) plane on each end of the crystal was the only shaping done to obtain the required aspect ratio.[6] The crystal ends, which were the contact surfaces, were subjected to neither etching nor polishing. A 2.1- × 2.1- × 4.1-mm^3 HgI_2 crystal was harvested, shaped, and fabricated into a Frisch collar detector. A palladium wire was attached to each end of the crystal with Aquadag E, which was also used as the contact material. The crystal was first coated with Parylene C to a thickness of ~40 mm. The purpose of this Parylene coating was to protect the crystal and strengthen the contact areas and wires. After being coated with Parylene C, the contact wire was further strengthened by application of an epoxy.

The Frisch collar detector was fabricated by wrapping the planar detector with a Teflon tape followed by a thin copper foil. The cross section of the Frisch collar device is shown in Fig. 4. The Frisch collar detector was tested in a test box placed in a Faraday cage. The ^{137}Cs source was placed inside the box near the cathode side of the detector. For the Frisch collar device testing, the cathode and the copper collar were grounded ($V_{cathode} = V_{collar} = 0$) while the anode was biased at $V_{anode} = 1500$ V. The planar detector configuration could be tested either before the crystal was fabricated into the Frisch collar detector or by disconnecting the Frisch collar or letting it float. Cesium-137 spectra were collected at the start of the bias application and after 24 h of bias application. The bias

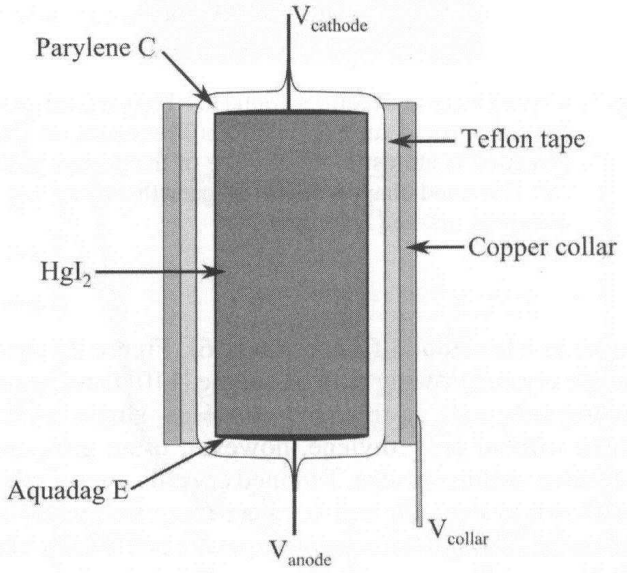

Fig. 4. The cross section of the HgI_2 Frisch collar device.

was continually supplied because of the polarization problem that usually plagued HgI_2 devices. The performance of HgI_2 devices has been shown to improve, and the devices reach their best energy resolutions after days or weeks of bias application.[28]

IV. RESULTS AND ANALYSIS

IV.A. Organics-Aided Growth of HgI_2

Crystal forms that usually appear in a vapor-grown HgI_2 crystal are the basal pinacoid (001), tetragonal prisms of the first order {110}, and pyramid of the second order {h0l} crystal forms or faces.[29,30] These crystal forms can be observed on a HgI_2 crystal grown by the vertical furnace method *without* the presence of any polyethylene (Fig. 5). The {110} faces feature diamond-shaped striae or growth layers, with the striae making a 45-deg angle to the (001) face.

The crystal forms and features found in a vertical furnace–grown HgI_2 can also be found in HgI_2 crystals

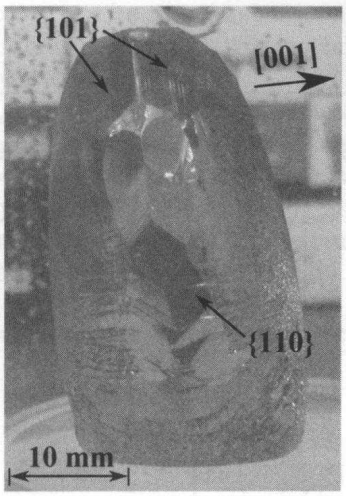

Fig. 5. Crystal faces and features found in a HgI_2 crystal grown by the vertical furnace method. The *c*-axis or [001] direction is almost to the surface of the growth pedestal. Diamond-shaped striae or growth layers can be observed on the {110} face.

grown in a horizontal furnace (Fig. 6). Figure 6a shows a single crystal growing with one of the {110} faces against the ampoule wall. In this study the HgI_2 single crystals grown *without* polyethylene, however, often grew only into cubic millimeter size. Twinned crystals, two of which are shown in Figs. 6b and 6c, were more frequently encountered. Though the crystal forms are not readily identifiable as in those in a single crystal, the striations seen on the crystal face in Fig. 6b suggest that the crystal face is that of the {110} crystal forms. Judging from the orientation of the striae, each twin grew in the direction of the *c*-axis or the [001] direction. Similar observations can be made on the crystal face shown in Fig. 6c. It appears that the type(s) of twinning shown in Fig. 6b is (are) either penetration twinning or cyclic twinning. Some of the twins in Fig. 6b appear to grow with their *c*-axes parallel to each other; i.e., the twins grew in parallel to one another (a polysynthetic twin). Other twins grew with their respective *c*-axis not in parallel to one another (either a cyclic twin or a penetration twin).

Crystals grown with the low $\overline{M}_w$ polyethylene, as shown in Fig. 7, have a more identifiable morphology of prismatic tetragonal and have identifiable crystal forms and faces. Figure 7a shows a single crystal growing with one of the {110} faces against the wall, while Fig. 7b shows two single crystals growing with one of the (001) faces right against the wall. In other words, the *c*-axis of the crystal in Fig. 7a is perpendicular to the radius of the ampoule, while the *c*-axis of the crystals in Fig. 7b is close to parallel to the radius of the ampoule. As seen in these Figs. 7a and 7b, the HgI_2 single crystals grown with the low $\overline{M}_w$ polyethylene have the fortuitous prismatic tetragonal shape that can be utilized and fabricated into Frisch collar detectors. Twinned crystals were still found, one of which is shown in Fig. 7c. The observed growth layers on one of the twins shown in Fig. 7c indicate that the face was one of the {110} faces, and hence, the *c*-axis of the twin could be determined. Unlike the twinned crystals grown in the absence of polyethylene, most of the twinned crystals that grew with polyethylene were cyclic twins (the *c*-axes of the twins in the cyclic twin are not parallel to one another). For the Frisch collar detector fabrication, each twin could be shaped into a tetragonal prism with a required aspect ratio simply by cleaving the crystal parallel to its (001) plane.

IV.B. HgI_2 Frisch Collar Detector

The $CCE(x)_{planar}$ and $CCE(x)_{Frisch}$ profiles for the HgI_2 device in the planar and Frisch collar device configurations, both detectors biased at 1500 V, are shown in Fig. 8 as a function of normalized length. These profiles were generated using $\mu_e\tau_e = 0.0008\ cm^2 \cdot V^{-1}$ and $\mu_h\tau_h = 0.00003\ cm^2 \cdot V^{-1}$. Notice that the $CCE(x)_{Frisch}$ profile is relatively flat (uniform) especially for almost three-fifths of the device length. In contrast, the $CCE(x)_{planar}$ profile is flat only near the cathode region (approximately between 0 and 0.1). A flat region in a *CCE* curve translates into counts within the same peak channel

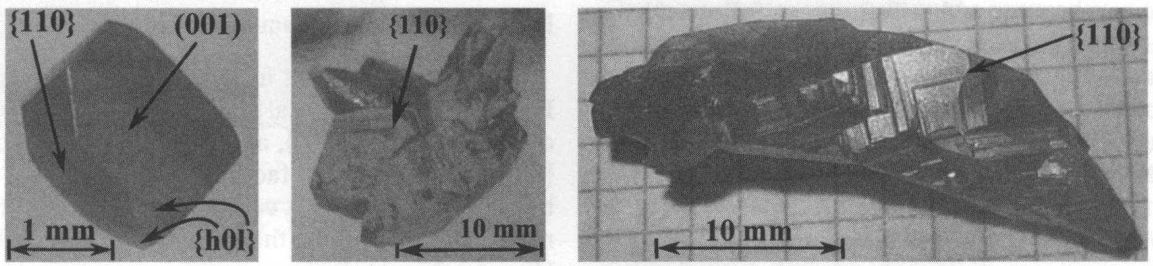

(a) (b) (c)

Fig. 6. HgI_2 crystals shown in (a), (b) and (c) were grown without polyethylene. Both crystals in (b) and (c) were twinned. Apparent in (b) are the growth layers indicative of the {110} crystal forms or faces. The growth layers indicating the {110} face are also apparent in (c).

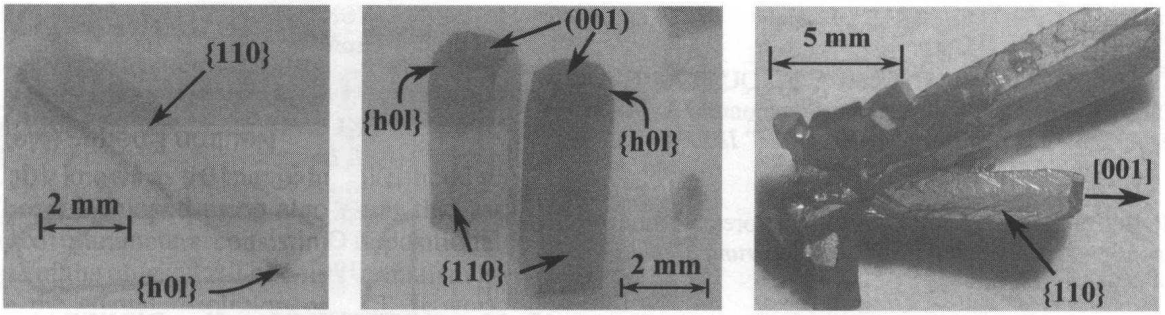

Fig. 7. HgI_2 crystals grown with low $\overline{M}_w$ polyethylene. (a) A single crystal grew with its *c*-axis perpendicular to the ampoule radius. (b) Two single crystals grew with their *c*-axes close to parallel to the ampoule radius. (c) Twinned crystals showing the striae or growth layers indicative of the {110} face, hence, also indicative of the direction of the *c*-axis.

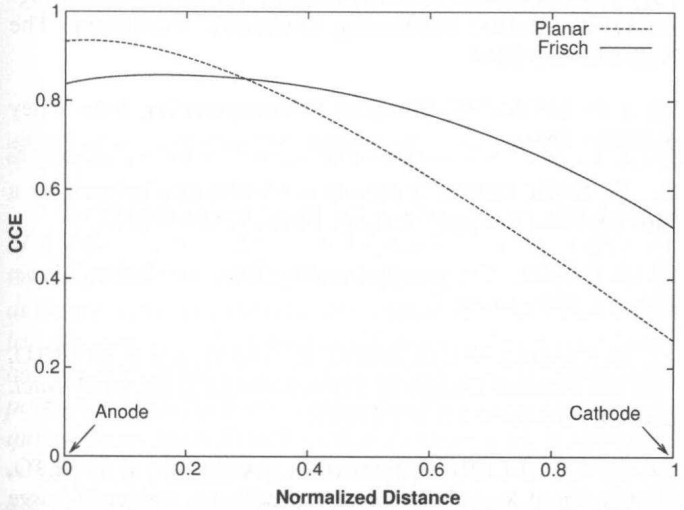

Fig. 8. The charge collection efficiency for the HgI_2 2.1- × 2.1- × 4.1-mm^3 device in the planar and the Frisch collar device configurations, respectively.

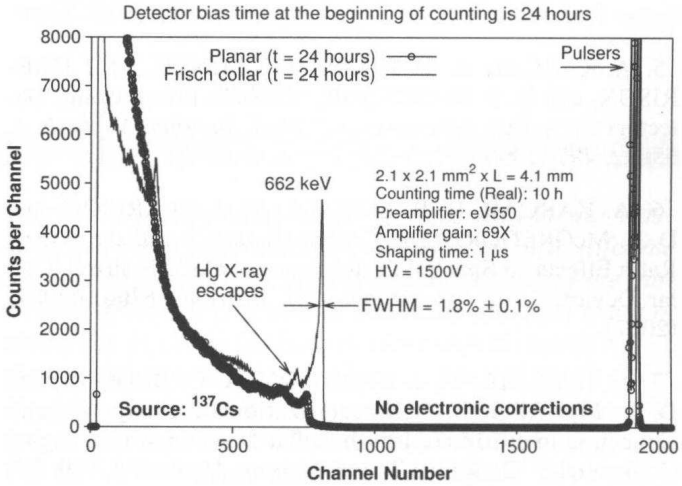

Fig. 9. The ^{137}Cs spectra taken with a HgI_2 detector in both the planar and the Frisch collar configurations.

number. Therefore, the longer the flat region in a *CCE* curve is, the more counts are observed for the photoelectric events in the corresponding photopeak channel.

Shown in Fig. 9 are two ^{137}Cs spectra, each taken with either the planar or the Frisch collar detector configurations of the same crystal. Each spectrum was collected for 10 h (real) of counting time after the detector (of the respective detector configuration) had been subjected to 1500-V bias for 24 h. No electronic correction was employed afterward. Apparent is the increased performance of the HgI_2 spectrometer due to the application of the Frisch collar. This improvement in performance with the Frisch collar is signified by the photopeak energy resolution of 1.8% at 662 keV and the appearance of other spectral features. The energy resolution remained constant even after the first 24 h of bias application, indicating that the HgI_2 Frisch collar detector could reach its optimal energy resolution considerably ahead of other reported HgI_2 detectors.

V. CONCLUSIONS

HgI_2 crystals grown by vapor in the presence of low M_w polyethylene have the fortuitous shape of parallelepiped or tetragonal prisms. This shape has allowed the application of the Frisch collar technology to improve the spectroscopic performance of the planar device. This improvement is achieved by the alteration of the weighting potential distribution within the device, which in turn reduces the contribution of the charge carriers with lower $\mu\tau$ product (holes) to the charge induction on the reading electrode. With only standard NIM equipment and without any electronic correction, a room-temperature Frisch collar HgI_2 spectrometer has been fabricated, yielding sub-2% energy resolution.

ACKNOWLEDGMENT

Funding is provided by the U.S. Department of Defense through Defense Threat Reduction Agency contract HDTRA-01-07-1-007.

REFERENCES

1. G. OTTAVIANI, C. CANALI, and A. A. QUARANTA, "Charge Carrier Transport Properties on Semiconductor Materials Suitable for Nuclear Radiation Detectors," *IEEE Trans. Nucl. Sci.*, **22**, 192 (1975).

2. G. GEORGESON and F. MILSTEIN, "Theoretical Study of the Dislocation Structure in HgI_2," *Nucl. Instrum. Methods A*, **285**, 488 (1989).

3. D. S. McGREGOR and R. A. ROJESKI, "Performance of CdZnTe Geometrically Weighted Semiconductor Frisch Grid Radiation Detectors," *IEEE Trans. Nucl. Sci.*, **46**, *3*, Part 1, 250 (1999).

4. W. J. McNEIL, D. S. McGREGOR, A. E. BOLOTNIKOV, G. W. WRIGHT, and R. B. JAMES, "Single-Charge-Carrier-Type Sensing with an Insulated Frisch Ring CdZnTe Semiconductor Radiation Detector," *Appl. Phys. Lett.*, **84**, 1988 (2004).

5. A. KARGAR, A. M. JONES, W. J. McNEIL, M. J. HARRISON, and D. S. McGREGOR, "CdZnTe Frisch Collar Detectors for γ-Ray Spectroscopy," *Nucl. Instrum. Methods A*, **558**, *2*, 497 (2006).

6. A. KARGAR, R. B. LOWELL, M. J. HARRISON, and D. S. McGREGOR, "The Crystal Geometry and the Aspect Ratio Effects on Spectral Performance of CdZnTe Frisch Collar Device," *Proc. Soc. Photo-Opt. Instrum.*, **6706**, 67061J (2007).

7. A. KARGAR, M. J. HARRISON, A. C. BROOKS, and D. S. McGREGOR, "Characterization of Charge Carrier Collection in a CdZnTe Frisch Collar Detector with a Highly Collimated ^{137}Cs Source," *Nucl. Instrum. Methods A*, **620**, 270 (2010).

8. M. SCHIEBER, I. BEINGLASS, G. DISHON, A. HOLZER, and G. YARON, "State-of-the-Art of Crystal Growth and Nuclear Spectroscopic Evaluation of Mercuric Iodide Radiation Detectors," *Nucl. Instrum. Methods*, **150**, 71 (1978).

9. H. SCHOLZ, "On Crystallization by Temperature-Gradient Reversal," *Acta Elec.*, **17**, 69 (1974).

10. A. E. BOLOTNIKOV, J. BAKER, R. DEVITO, J. SANDOVAL, and L. SZURBART, "HgI_2 Detector with a Virtual Frisch Ring," *IEEE Trans. Nucl. Sci.*, **52**, 468 (2005).

11. S. P. FAILE, A. J. DABROWSKI, G. C. HUTH, and J. S. IWANCZYK, "Mercuric Iodide (HgI_2) Platelets for X-Ray Spectroscopy Produced by Polymer Controlled Growth," *J. Cryst. Growth*, **50**, *3*, 752 (1980).

12. A. BURGER, M. ROTH, and M. SCHIEBER, "The Role of Polyethylene in Platelet Growth of Mercuric Iodide," *J. Cryst. Growth*, **56**, 526 (1982).

13. A. BURGER, A. LEVI, J. NISSENBAUM, M. ROTH, and M. SCHIEBER, "Yield and Quality of HgI_2 Vapor Grown Platelets," *J. Cryst. Growth*, **72**, 643 (1985).

14. J. LASKOWSKI, H. KUC, K. CONDER, and J. PRZYŁUSKI, "Growth of α-HgI_2 Platelets," *Mat. Res. Bull.*, **22**, *6*, 715 (1987).

15. J. PRZYŁUSKI and J. LASKOWSKI, "α-HgI_2 Platelets Technology," *Nucl. Instrum. Methods A*, **283**, 144 (1989).

16. G. A. JEFFREY and M. VLASSE, "On Crystal Structures of Red Yellow and Orange Forms of Mercuric Iodide," *Inorg. Chem.*, **6**, *2*, 396 (1967).

17. M. HOSTETTLER, H. BIRKEDAL, and D. SCHWARZENBACH, "Polymorphs and Structures of Mercuric Iodide," *CHIMIA*, **55**, *6*, 541 (2001).

18. C. GUMINSKI, "The Hg-I (Mercury-Iodine) System," *J. Phase Equi.*, **1B**, 206 (1997).

19. T. HAHN, U. SHMUELI, A. J. C. WILSON, and I. U. OF CRYSTALLOGRAPHY, *International Tables for Crystallography*, D. Reidel Publishing Company, Dordrecht, The Netherlands(1984).

20. J. D. JACKSON, *Classical Electrodynamics*, John Wiley & Sons (1999).

21. W. SHOCKLEY, "Currents to Conductors Induced by a Moving Point Charge," *J. Appl. Phys.*, **9**, 635 (1938).

22. S. RAMO, "Currents Induced by Electron Motion," *Proc. IRE*, **27**, 584 (1939).

23. G. CAVALLERI, G. FABRI, E. GATTI, and V. SVELTO, "On the Induced Charge in Semiconductor Detectors," *Nucl. Instrum. Methods*, **21**, 177 (1963).

24. G. CAVALLERI, G. FABRI, E. GATTI, and V. SVELTO, "Extension of Ramo's Theorem as Applied to Induced Charge in Semiconductor Detectors," *Nucl. Instrum. Methods*, **92**, 137 (1971).

25. D. S. McGREGOR and R. A. ROJESKI, "High-Resolution Ionization Detector and Array of Such Detectors," U.S. Patent 6,175,120 (Jan. 2001).

26. V. RADEKA, "Low-Noise Techniques in Detectors," *Ann. Rev. Nucl. Part. Sci.*, **38**, 217 (1988).

27. H. A. LAMONDS, "Review of Mercuric Iodide Development Program in Santa Barbara," *Nucl. Instrum. Methods*, **213**, 5 (1983).

28. V. GERRISH, "Polarization and Gain in Mercuric Iodide Gamma-Ray Spectrometers," *Nucl. Instrum. Methods A*, **322**, 402 (1992).

29. I. NICOLAU, "Solution Growth of Sparingly Soluble Single-Crystals from Soluble Complexes. II. Growth of α-HgI_2 Single Crystals from Iodomercurate Complexes," *J. Cryst. Growth*, **48**, 51 (1980).

30. E. S. DANA and W. E. FORD, *A Textbook of Mineralogy*, John Wiley & Sons (1932).